HHS Public Access

Author manuscript

J Comp Neurol. Author manuscript; available in PMC 2017 June 15.

Published in final edited form as:

J Comp Neurol. 2017 June 15; 525(9): 2075–2089. doi:10.1002/cne.24171.

Ultrastructural Analysis of Parvalbumin Synapses in Human Dorsolateral Prefrontal Cortex

Jill R. Glausier[1], **Rosalinda C. Roberts**[2], and **David A. Lewis**[1,3]

[1]Department of Psychiatry, University of Pittsburgh School of Medicine, Pittsburgh, PA 15213

[2]Department of Psychiatry and Behavioral Neurobiology, University of Alabama at Birmingham, Birmingham, AL 35294

[3]Department of Neuroscience, University of Pittsburgh School of Arts and Sciences, Pittsburgh, PA 15213

Abstract

Coordinated activity of neural circuitry in the primate dorsolateral prefrontal cortex (DLPFC) supports a range of cognitive functions. Altered DLPFC activation is implicated in a number of human psychiatric and neurological illnesses. Proper DLPFC activity is, in part, maintained by two populations of neurons containing the calcium-binding protein parvalbumin (PV): local inhibitory interneurons that form Type II synapses, and long-range glutamatergic inputs from the thalamus that form Type I synapses. Understanding the contributions of each PV neuronal population to human DLPFC function requires a detailed examination of their anatomical properties. Consequently, we performed an electron microscopic analysis of 1) the distribution of PV immunoreactivity within the neuropil, 2) the properties of dendritic shafts of PV-IR interneurons, 3) Type II PV-IR synapses from PV interneurons, and 4) Type I PV-IR synapses from long-range projections, within the superficial and middle laminar zones of the human DLPFC. In both laminar zones, Type II PV-IR synapses from interneurons comprised ~60% of all PV-IR synapses, and Type I PV-IR synapses from putative thalamocortical terminals comprised the remaining ~40% of PV-IR synapses. Thus, the present study suggests that innervation from PV-containing thalamic nuclei extends across superficial and middle layers of the human DLPFC. These findings contrast with previous ultrastructural studies in monkey DLPFC where Type I PV-IR synapses were not identified in the superficial laminar zone. The presumptive added

Corresponding author: Jill R. Glausier, PhD, Department of Psychiatry, Western Psychiatric Institute and Clinic University of Pittsburgh Biomedical Science Tower, Room W1654 Tel: 412-624-7869; Fax: 412-624-9910 glausierjr@upmc.edu.

DATA ACCESSBILITY

All data associated with this manuscript is presented in the submission.

CONFLICT OF INTEREST

David A. Lewis currently receives investigator-initiated research support from Pfizer. In 2013–2015, he served as a consultant in the areas of target identification and validation and new compound development to Autifony, Bristol-Myers Squibb, Concert Pharmaceuticals and Sunovion. Jill R. Glausier and Rosalinda C. Roberts have no conflicts of interest.

ROLE OF AUTHORS

All authors had full access to all the data in the study and take responsibility for the integrity of the data and the accuracy of the data analysis. Study concept and design: JRG, DAL, RCR. Acquisition of data: JRG. Analysis and interpretation of data: JRG, DAL. Drafting of the manuscript: JRG. Critical revision of the manuscript for important intellectual content: DAL, RCR. Statistical analysis: JRG. Obtained funding: DAL, RCR. Administrative, technical, and material support: DAL, RCR. Study supervision: DAL.

modulation of DLPFC circuitry by the thalamus in human may contribute to species-specific, higher-order functions.

Graphical Abstract

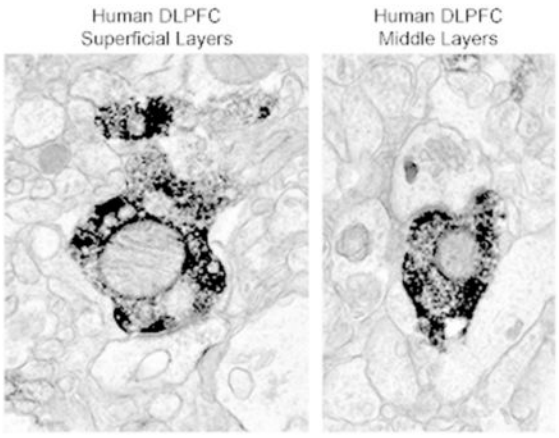

Keywords

Electron microscopy; Axon Terminal; GABA; Mediodorsal Thalamus; Cortical Layers; AB_477329; AB_10000343

INTRODUCTION

Working memory, a core cognitive domain (Baddeley, 1992), is altered in a number of psychiatric and neurologic illnesses, including schizophrenia (Barch and Ceaser, 2012; Lewis et al., 2012), autism spectrum disorder (O'Hearn et al., 2008; Zikopoulos and Barbas, 2013), and Alzheimer's disease (Germano and Kinsella, 2005; Jahn, 2013). Working memory ability in human and non-human primates depends upon the coordinated activation of a distributed neural circuit that includes the dorsolateral prefrontal cortex (DLPFC) (Petrides, 2005; Arnsten and Jin, 2014) and the mediodorsal (MD) nucleus of the thalamus (Constantinidis and Procyk, 2004; Watanabe and Funahashi, 2012). The DLPFC-MD thalamus circuitry important for working memory includes two types of neurons that contain the calcium-binding protein parvalbumin (PV): local GABAergic interneurons within the DLPFC and long-range glutamatergic afferent inputs from the MD thalamus to the DLPFC.

In the human and non-human primate DLPFC, PV interneuron somata and dendritic and axonal processes are predominately located in layers 3 – 4, and the latter form Gray's Type II synapses (Hof et al., 1991; Williams et al., 1992; Conde et al., 1994; Woo et al., 1997; Melchitzky et al., 1999; Lewis et al., 2001). Previous ultrastructural analyses in monkey DLPFC demonstrated that in both the middle (layers deep 3 – 4) and superficial (layers 2 – superficial 3) laminar zones, PV interneurons synapse onto pyramidal cell dendritic shafts, spines, somata, and axon initial segments (Williams et al., 1992; Melchitzky et al., 1999).

In monkeys, the MD thalamus provides robust, direct afferent inputs to the DLPFC (Kievit and Kuypers, 1977; Goldman-Rakic and Porrino, 1985; Giguere and Goldman-Rakic, 1988; Barbas et al., 1991; Erickson and Lewis, 2004; Negyessy and Goldman-Rakic, 2005). Indeed, the majority of all thalamic input to the monkey DLPFC arises from the MD nucleus of the thalamus (Barbas et al., 1991), and these afferents exuberantly target the middle cortical layers, with sparse and rarely identified afferents in the superficial and deep laminar zones (Giguere and Goldman-Rakic, 1988; Barbas et al., 1991; Erickson and Lewis, 2004; Negyessy and Goldman-Rakic, 2005). The axon terminals of MD thalamic projections: 1) contain PV (Munkle et al., 1999; Negyessy and Goldman-Rakic, 2005); 2) are glutamatergic (Pirot et al., 1994); 3) form Gray's Type I synapses (White, 1986) predominately onto pyramidal cell spines (Melchitzky et al., 1999; Negyessy and Goldman-Rakic, 2005); and 4) form those synapses exclusively within in the middle laminar zone (layers deep 3 – 4) (Williams et al., 1992; Melchitzky et al., 1999; Negyessy and Goldman-Rakic, 2005).

Although the ultrastructural properties of PV thalamocortical and PV interneuron synapses in the monkey DLPFC have been carefully characterized as described above (Williams et al., 1992; Melchitzky et al., 1999; Negyessy and Goldman-Rakic, 2005), no such characterization exists for the human DLPFC. These data are important to acquire in order to appropriately design and interpret anatomical and functional studies of human DLPFC in disease states. Moreover, the use of experimental and anatomical studies in other species to understand the impact of PV synaptic alterations in human disease requires knowledge of the extent to which non-human anatomy reflects that of human. Indeed, differences exist between human and non-human primates in prefrontal cortex (PFC) anatomy and PFC-mediated behaviors (Passingham, 2008; Vendetti and Bunge, 2014; Silbereis et al., 2016). Consequently, we performed an electron microscopic ultrastructural analysis of PV axonal terminals forming Type I or Type II synapses (putative thalamocortical and interneuron terminals, respectively) in the superficial and middle laminar zones of the human DLPFC.

MATERIALS AND METHODS

Human Subjects

Brain specimens were obtained from two sources: the Maryland Brain Collection and the University of Pittsburgh. The Maryland Brain Collection cases (N=2) were obtained with family permission, and autopsies were performed in the Office of the Chief Medical Examiner of Maryland (Roberts et al., 2005). The University of Maryland Institutional Review Board approved all procedures. The University of Pittsburgh cases (N=2) were obtained during autopsies performed at the Allegheny County Medical Examiner's Office (Pittsburgh, PA) after consent for donation was obtained from the next-of-kin. All procedures were approved by the University of Pittsburgh's Committee for the Oversight of Research and Clinical Training Involving the Dead, and the Institutional Review Board for Biomedical Research. Information regarding the Maryland Brain Collection cases was gathered from medical records, family interviews, and autopsy reports (Roberts et al., 2005). Information regarding the University of Pittsburgh cases was also gathered from these sources, and an independent committee of experienced research clinicians confirmed the absence of psychiatric diagnoses (Volk et al., 2012). Subjects were selected based on the

absence of any known psychiatric or neurological diagnoses and the presence of short postmortem intervals in order to obtain optimal ultrastructural preservation. Subject characteristics are detailed in Table 1.

Tissue Preparation

For the Maryland Brain Collection cases, ~1cm-thick coronal blocks of left hemisphere Brodmann area 9 were immersed in a cold solution of 4% paraformaldehyde and 1% glutaraldehyde for at least one week at 4oC. Vibratome sections (40μm) were stored in cold 0.1M phosphate buffer (PB) (Roberts et al., 2005). For the University of Pittsburgh cases, ~1cm-thick coronal blocks of left hemisphere Brodmann area 9 were immersed in a solution of 4% paraformaldehyde and 0.2% glutaraldehyde for 24 hours at room temperature, followed by 24 hours at 4°C. Vibratome sections (50μm) were stored in cryoprotectant at −30°C. Qualitative examination generally showed better ultrastructural preservation in samples fixed for 48 hours than for one week.

Immunohistochemistry

Maryland Brain Collection cases—Single-label immunoperoxidase labeling was performed as previously described (Roberts et al., 2005). Briefly, tissue sections were incubated in 1% sodium borohydride, then 1.5% H_2O_2. Sections were then placed in a 10% horse serum blocking solution, and incubated at 4°C overnight in a 1.5% horse serum blocking solution containing mouse anti-PV (Sigma-Aldrich, St. Louis, MO) diluted at 1:10,000. On the following day, sections were incubated in biotinylated horse anti-mouse (1:250), then in avidin-biotin-peroxidase complex (ABC, Elite kit, Vector, Burlingame, CA). Bound peroxidase was visualized by treating sections with 3,3′-diaminodenzidine (DAB) containing 0.03% H_2O_2. Post-fixation in 1% osmium tetroxide, *en bloc* staining with uranyl acetate, dehydration in ascending ethanols and propylene oxide, and embedding in Epon resin was performed.

University of Pittsburgh cases—Tissue was processed as previously described (Melchitzky et al., 1999). Briefly, tissue sections were incubated in 1.0% sodium borohydride, then 1.0% H_2O_2. Sections were then placed in blocking solution containing 0.2% bovine serum album, 0.04% Triton X-100, 3% normal horse serum, and 3% normal human serum; and then incubated at 4°C overnight in blocking solution also containing mouse anti-PV (Swant, Switzerland) diluted at 1:5,000. On the following day, sections were incubated in biotinylated horse anti-mouse (1:400), then in ABC. Bound peroxidase was visualized by treating sections with DAB containing 0.003% H_2O_2. Post-fixation in 2% osmium tetroxide, dehydration in ascending ethanols and propylene oxide, and embedding in Epon resin was performed.

Antibody Characterization—Table 2 details the two primary antibodies used in these studies. Tissue sections processed as described, but in which the primary antibody was omitted, showed no evidence of specific labeling at the light and/or electron microscopic levels. This indicates that the secondary antibodies used did not generate background labeling. The mouse anti-PV antibody from Sigma-Aldrich recognizes a single band at a molecular weight of approximately 12kDa in immunoblot analysis (Celio, 1986; Park et al.,

2008), and does not cross react with GABA or glutamate (Celio, 1986). Labeling is abolished after preadsorption with purified PV protein (Hackney et al., 2005). The mouse anti-PV antibody from Swant specifically labels the ^{45}Ca-binding spot of PV in a two-dimensional immunoblot, and all specific labeling is abolished in PV knockout mice (Celio et al., 1988; Schwaller et al., 1999). The expected pattern of labeling for both primary anti-PV antibodies (Hof et al., 1991; Melchitzky et al., 1999; Glausier et al., 2009) was seen at the light microscopic level in the current study. Qualitative examination showed similar levels of PV immunoreactivity in all subject samples.

Analysis of Material

Samples from the superficial (layers 2 - superficial 3) and middle (layers deep 3 – 4) zones of the DLPFC (Figure 1A) were taken from the same tissue section per subject, cut in 85nm-thick ultrathin serial sections, collected on Formvar-coated copper slot grids (Electron Microscopy Sciences, Hatfield, PA), and examined on a JEOL JEM 1011 TEM. To assess the presence of PV immunoreactivity within the neuropil, 50 fields were imaged at X25,000 over 2 – 6 ultrathin sections cut in series for each subject and within each laminar zone. Thus, on the first ultrathin section in the series, 50 distinct fields were imaged based on ultrastructural preservation and presence of PV immunoreactivity, and the same regions were then photographed on all subsequent sections in the series. In the superficial laminar zone, 270 PV-immunoreactive (-IR) profiles were identified, and each subject contributed an average of 68 ± 31 profiles. In the middle laminar zone, 432 PV-IR profiles were identified, and each subject contributed 108 ± 54 profiles. For axon terminal and mitochondrial analyses, 25 PV-IR terminals were identified for each laminar zone within each subject (n=100 PV-IR terminals/laminar zone), and examined over 2–6 ultrathin sections cut in series. On the first ultrathin section in the series, a putative PV-IR terminal was identified and photographed at X25,000. The same region was then photographed at the same magnification on all subsequent sections in the series. These images were then used to 1) confirm the PV-IR profile as an axon terminal, 2) determine whether and what type of synapse was present, and 3) count the number of mitochondria present in the axon terminals. To analyze putative pyramidal cell axon terminals, 25 non-PV-IR axon terminals in each laminar zone within each subject (n=100 non-PV-IR terminals/laminar zone) were randomly selected using a random number generator, and examined across the serial sections. This type of axon terminal analysis was performed so that synapses, structures, and organelles could be accurately identified and counted only once. Neuronal profiles, mitochondria, and synapses were identified using established criteria (Peters et al., 1991). Any labeled elements that could not be identified based on these criteria were classified as unknown, and excluded from analysis (Bordelon et al., 2005). The representative electron micrographs presented in the current manuscript have been digitally altered to increase contrast.

The types of neuronal profiles immunoreactive for PV within the neuropil from the Maryland Brain Collection that were labeled with mouse anti-PV (Sigma-Aldrich), and subjects from the University of Pittsburgh that were labeled with mouse anti-PV (Swant) was compared using a Fisher’s exact test since expected counts were less than five for some categories of neuronal profiles. Chi-square analysis was used to compare the distribution of labeled neuronal profiles and presence of mitochondria in axonal terminals in superficial and

middle laminar zones in the total cohort of four subjects. Independent sample t-tests were used to compare the number of mitochondria in PV-IR and non-PV-IR axon terminals.

RESULTS

Light Microscopic Distribution of PV in Human DLPFC

At the light microscopic level (Figure 1), qualitative examination of PV immunoreactivity in the human DLPFC showed expected labeling of PV interneuron somata and processes in both the superficial (Figure 1B–C) and middle (Figure 1D–E) laminar zones, but PV-IR boutons from unknown neurons were prevalent throughout the neuropil of both laminar zones. To determine the extent to which the PV-IR boutons in human DLPFC reflected axon terminals, the type of synapse formed, and the postsynaptic target, quantitative immunoelectron microscopic analyses were performed.

Neuropil Distribution of PV Immunoreactivity in Human DLPFC

Immunoreactivity for PV was identified in all components of the neuropil, including axon terminals, pre-terminal axons, dendritic shafts, and dendritic spines in both superficial and middle laminar zones (Figure 2). Qualitative analyses indicated that in both laminar zones, PV labeling was most commonly seen in dendritic shafts and least commonly identified in dendritic spines, consistent with the specific localization of PV to largely aspiny, GABAergic neurons (Celio, 1986; Conde et al., 1994). Quantitative analysis demonstrated that the proportion of different neuronal profiles immunoreactive for PV did not differ based on antibody used in either laminar zone (Figure 3A–B). As such, the data for all four subjects were combined for the remaining analyses. The proportion of different neuronal profiles immunoreactive for PV did not differ in superficial relative to middle laminar zones in the human DLPFC (χ^2=6.5, p=0.2; Figure 3C).

PV-IR Dendritic Shafts in Human DLPFC

In both superficial and middle laminar zones, ~50% of PV-IR profiles were dendritic shafts (Figure 3). As expected PV-IR dendrites typically exhibited DAB labeling that filled the profile, though microtubules, mitochondria, and/or small vesicles could be identified. Many PV-IR dendritic profiles received one or more Type I synapses from an unlabeled axon terminal (Figure 2B, D). In the superficial laminar zone, 28% (38 of 138) of PV-IR dendritic profiles received Type I synapses, and 32% (12 of 38) of those PV-IR dendritic profiles received more than one Type I synapse. In the middle laminar zone, 39% (83 of 211) of PV-IR dendritic profiles received Type I synapses, and 29% (24 of 83) of those PV-IR dendritic profiles received more than one Type I synapse. None of the 138 PV-IR dendrites analyzed in the superficial laminar zone were innervated by PV-IR axon terminals, and only 1.4% (3 of 211) of PV-IR dendritic profiles in the middle laminar zone were innervated by a PV-IR axon terminal (Figure 2D).

PV-IR Axon Terminals in Human DLPFC

Superficial Laminar Zone—In the superficial laminar zone, 22% of PV-IR profiles were axon terminals (Figure 3). As expected, PV-IR terminals typically exhibited DAB labeling that filled the profile (Figure 4A–C, Figure 5A–C). Of the 100 PV-IR terminals analyzed

across serial ultrathin sections, 48% formed identifiable synapses, and unexpectedly, these included both Type I and Type II (Table 3). PV-IR Type I synapses were exclusively formed on dendritic spines, whereas Type II synapses primarily targeted dendritic shafts (Table 4). One or more mitochondria were present in 76% of all PV-IR terminals examined. In contrast, only 45% of 100 randomly selected non-PV-IR axon terminals from the same fields contained one or more mitochondrion. Chi-square analysis demonstrated that significantly fewer non-PV-IR axon terminals contained mitochondria than PV-IR terminals (χ^2=20.1, p<0.00001; Table 5). The mean number of mitochondria present in axon terminals was significantly higher (t=5.7, p<0.001) in PV-IR axon terminals (0.98 ± 0.75) than non-PV-IR axon terminals (0.46 ± 0.52).

Middle Laminar Zone—In the middle laminar zone, 18% of PV-IR profiles were axon terminals (Figure 3). As expected, PV-IR terminals typically exhibited DAB labeling that filled the profile (Figure 4D–G, Figure 5D–G), and included PV-IR boutons that were of the *en passant* type (Figure 2F). Of the 100 PV-IR terminals analyzed across serial ultrathin sections, 57% formed identifiable synapses, including both Type I and Type II synapses. Two of the 57 terminals formed two synapses, for a total of 59 identifiable synapses (Table 3). Type I synapses were formed onto dendritic spines and shafts, including PV-IR dendrites. Type II synapses were also formed onto pyramidal cell somata and axon initial segments (Table 4). One or more mitochondria were present in 73% of all PV-IR terminals examined. In contrast, only 39% of 100 randomly selected non-PV-IR axon terminals from the same fields contained one or more mitochondrion. Chi-square analysis demonstrated that significantly fewer non-PV-IR axon terminals contained mitochondria than PV-IR terminals (χ^2=23.5, p<0.00001; Table 5). The mean number of mitochondria present in axon terminals was significantly higher (t=5.6, p<0.001) in PV-IR axon terminals (0.95 ± 0.8) than non-PV-IR axon terminals (0.41 ± 0.53).

DISCUSSION

We performed qualitative and quantitative immuno-electron microscopic analyses of PV-IR neuronal profiles and synapses in the DLPFC of four human subjects without any brain diseases using 1) two different mouse monoclonal antibodies raised against PV, 2) human tissue collected at two different sites, and 3) two distinct laminar zones that were previously reported to show differences in PV synaptology in monkey DLPFC (Williams et al., 1992; Melchitzky et al., 1999). The neuronal profile localization of PV immunoreactivity did not differ within a laminar zone as a function of antibody or tissue source, demonstrating the precision and reliability of the current findings.

Characteristics of mitochondria in PV-IR and non-PV-IR axon terminals

In both the superficial and middle laminar zones of the human DLPFC, ~40% of non-PV-IR terminals and ~75% of PV-IR terminals analyzed in series contained one or more mitochondria. Moreover, PV-IR axon terminals contained twice as many mitochondria as non-PV-IR axon terminals. These findings are consistent with previous results in the monkey and rodent PFC demonstrating that PV-IR thalamocortical glutamatergic terminals forming Type I synapses, and local PV GABAergic terminals forming Type II synapses, contain more

mitochondria than axon terminals lacking PV immunoreactivity (Negyessy and Goldman-Rakic, 2005; Gulyas et al., 2006; Fitzgerald et al., 2012; Takacs et al., 2015). The higher prevalence of mitochondria in axon terminals from PV neurons relative to putative pyramidal cell axon terminals likely reflects the substantial energy demands required to support firing of PV interneurons (Kann et al., 2014) and long-range thalamocortical inputs (Gil et al., 1999; but see Schoonover et al., 2014). Of note, the present analysis may underestimate the number of mitochondria in both PV-IR and non-PV-IR terminals given that complete three-dimensional reconstruction was not performed.

PV-IR Type II synapses in the human DLPFC: laminar and ultrastructural properties

In both laminar zones, the majority of PV-IR axon terminals forming identifiable synapses made Type II GABAergic synapses, and ~50% of these were onto dendritic shafts. Interestingly, dendritic spines are largely absent within the first ~100μm of apical dendritic shafts and ~50μm of basilar dendritic shafts of PFC pyramidal cells in monkey (Medalla and Luebke, 2015), and Type II synapses onto these proximal dendrites are prevalent (DeFelipe and Farinas, 1992; Williams et al., 1992; Lund and Lewis, 1993). Although the present study cannot definitively identify dendritic shafts as pyramidal or non-pyramidal, ~75% of cortical neurons are pyramidal cells (Hendry et al., 1987; Hornung and DeTribolet, 1994) which have extensive apical and basilar dendritic trees (Amatrudo et al., 2012). Moreover, nearly all targeted dendritic shafts were PV-negative (Table 4). Together, these data suggest that PV GABA inputs preferentially target proximal pyramidal cell dendritic shafts in the superficial and middle layers of the human DLPFC. Moreover, ~20% of PV-IR Type II synapses in both laminar zones targeted unlabeled, presumed pyramidal cell, somata. As GABA synapses at somata and proximal dendritic shafts powerfully inhibit pyramidal cell output in a precise temporal manner (Kubota et al., 2016), the current anatomical data support a role for strong PV interneuron inhibition of pyramidal cell output in the superficial and middle laminar zones of the human DLPFC.

The predominance of Type II synapses in both laminar zones is consistent with previous ultrastructural studies in the monkey DLPFC (Williams et al., 1992; Melchitzky et al., 1999), though there may exist subtle differences in the frequency of certain types of postsynaptic targets between species, DLPFC cortical area, and cortical layers (Williams et al., 1992; Melchitzky et al., 1999). For example, in the middle laminar zone in both monkey (Melchitzky et al., 1999) and human DLPFC area 9, ~30% of PV-IR Type II synapses were onto unlabeled somata or axon initial segments. However, in the same region and layer, 41% of PV-IR Type II synapses were onto dendritic spines in monkey (Melchitzky et al., 1999), whereas only 14% of PV-IR Type II synapses innervated dendritic spines in human. As GABA synapses onto spines affect synaptic integration within individual axo-spinous glutamatergic synapses (Chiu et al., 2013; Kubota et al., 2015), these data may indicate a larger role for PV Type II inputs in axo-spinous synaptic integration in the monkey than in the human.

Thalamocortical inputs: PV-IR Type I synapses

The identified PV Type I synapses in the human DLPFC most likely reflect thalamocortical inputs. For example, PV Type I synapses are unlikely to arise from cortical glutamatergic

pyramidal cells, which provide the majority of all glutamatergic synapses in the DLPFC (reviewed in DeFelipe et al., 2002; Elston, 2003), as numerous studies have failed to find PV-IR pyramidal cells (Blümcke et al., 1990; Baimbridge et al., 1992; Williams et al., 1992; Lund and Lewis, 1993; Conde et al., 1994; Gabbott and Bacon, 1996; DeFelipe, 1997; Sherwood et al., 2009). To our knowledge, two studies have found PV immunoreactivity in pyramidal cells of primates, but this labeling was typically weak and exclusive to the somata and proximal dendritic processes of Betz cells and layer 5 pyramidal cells in the primary motor, visual, and somatosensory cortices (Preuss and Kaas, 1996; Ichinohe et al., 2004). In non-primate species, PV-IR pyramidal-like cells have also been described in the canine hippocampal formation and cortex (Hof et al., 1996a; Hof et al., 1996b), and the echidna cortex (Hof et al., 1999). Other sources of Type I inputs in the DLPFC include the amygdala and the thalamus. The PV-IR Type I synapses identified in the current study are also unlikely to arise from the amygdala, as the DLPFC receives sparse input from the amygdala (Barbas and De Olmos, 1990; Miyashita et al., 2007), and PV immunoreactivity within the amygdala appears to be largely restricted to local circuit neurons (Sorvari et al., 1995; Mascagni et al., 2009). However, substantial evidence across multiple species indicates that cortical PV Type I synapses originate from the thalamus (Freund et al., 1985; Freund et al., 1989; Jones and Hendry, 1989; Blümcke et al., 1991; DeFelipe and Jones, 1991; del Río and DeFelipe, 1994; Molinari et al., 1995; Jones, 1998b; Negyessy and Goldman-Rakic, 2005; Familtsev et al., 2016). Thus, although the present study cannot definitively determine that these are exclusively thalamocortical synapses, substantial evidence supports this interpretation.

Three PV-containing thalamic nuclei project to the monkey DLPFC: MD, pulvinar, and ventral anterior (Jones and Hendry, 1989; Barbas et al., 1991; Munkle et al., 1999). The MD nucleus is the primary source of thalamic afferents into the DLPFC, and these exuberantly target the middle cortical layers, with sparse and rarely identified afferents in layers 2 – superficial 3 and layers 5 – 6 (Giguere and Goldman-Rakic, 1988; Barbas et al., 1991; McFarland and Haber, 2002; Erickson and Lewis, 2004; Negyessy and Goldman-Rakic, 2005). Projections from the pulvinar predominately innervate the middle layers, but may have sparse projections located in DLPFC layer 1 (Barbas et al., 1991; Romanski et al., 1997; Gutierrez et al., 2000). PV-containing projections from the ventral anterior nucleus predominately innervate middle and deep layers, but do have sparse projections located in layers 1- superficial 3 (Zikopoulos and Barbas, 2007). Together, these light microscopic studies indicate that the majority of PV-IR thalamocortical afferents to the monkey DLPFC target the middle laminar zone. Moreover, Type I synapses from the MD thalamus to the DLPFC have been identified in the middle laminar zone (Negyessy and Goldman-Rakic, 2005), and two previous ultrastructural studies of the monkey DLPFC failed to find PV Type I synapses in the superficial laminar zone (Williams et al., 1992; Melchitzky et al., 1999). As such, we hypothesized that PV Type I synapses would be exclusively identified in the middle laminar zone of the human DLPFC. Unexpectedly, we found that ~40% of PV-IR axon terminals forming identifiable synapses in both the middle and superficial laminar zones were Type I.

PV-IR Type I synapses in the human DLPFC: laminar and ultrastructural properties

In the middle laminar zone, 39% of PV-IR synapses were Type I, and these targeted dendritic spines and shafts roughly equally (52% and 48%, respectively). These findings differ from those in the human temporal pole, where 81% of PV-IR axon terminals in the middle laminar zone formed Type I synapses, and these terminals appear to target spines more frequently than dendritic shafts (del Río and DeFelipe, 1994). These findings also contrast with those in the middle laminar zone of monkey DLPFC area 9 where 52% of PV-IR axon terminals formed Type I synapses, and ~80% of these terminals targeted dendritic spines (Melchitzky et al., 1999). Finally, the current results also differ from the rat PFC where 98% of synapses from mediodorsal thalamocortical axon terminals targeted dendritic spines (Rotaru et al., 2005). In the human, 13% of the dendritic shafts receiving PV-IR Type I synapses were PV-IR, in agreement with previous qualitative findings in the monkey DLPFC (Melchitzky et al., 1999; Negyessy and Goldman-Rakic, 2005). However, this pattern of innervation is different from the rat PFC, where the majority of targeted dendritic shafts are PV-IR (Rotaru et al., 2005). Together, these comparisons suggest that thalamocortical inputs to the middle cortical layers can differentially regulate local pyramidal cells and interneurons across regions and species.

In the superficial laminar zone, 44% of PV-IR axon terminals forming identifiable synapses made Type I synapses, and these exclusively targeted dendritic spines. Thus, in the human DLPFC, putative PV thalamocortical synapses are present and prevalent across layers 2 – 4. Whether this finding represents a broader synaptic innervation zone of the MD thalamus, or if superficial layer synaptic inputs from the pulvinar and ventral anterior nucleus are more common in humans, remains to be determined. Interestingly, this finding contrasts with previous ultrastructural studies that did not observe PV-IR Type I synapses in the superficial laminar zone of monkey DLPFC area 9 (Melchitzky et al., 1999) or area 46 (Williams et al., 1992), and with existing light microscopic studies of monkey DLPFC indicating sparse thalamocortical afferents in the superficial laminar zone comprising layers 2 – superficial 3 (Giguere and Goldman-Rakic, 1988; Barbas et al., 1991; McFarland and Haber, 2002; Erickson and Lewis, 2004; Zikopoulos and Barbas, 2007). For example, ~20% of all ventral anterior thalamocortical afferent boutons in monkey DLPFC area 9 are located in the in the superficial laminar zone, and of those, only ~15% are PV-IR (Zikopoulos and Barbas, 2007). Thus, the existing data suggest that PV-IR thalamocortical inputs to the DLPFC differ across species, such that afferent axons are largely restricted to the middle laminar zone in monkey DLPFC, but PV-IR thalamocortical synapses in the human DLPFC extend across superficial and middle layers. Indeed, quantitative differences in putative thalamocortical inputs have been identified between human and non-human primate species in other cortical regions (Preuss et al., 1999; Preuss and Coleman, 2002; Garcia-Marin et al., 2013), including differences in the laminar distribution of presumed thalamic axonal boutons (Garcia-Marin et al., 2013).

The role of PV thalamocortical inputs

In sensory cortices, the middle laminar zone is innervated by “core” PV-IR neurons from anatomically defined first order thalamic nuclei, and these inputs are proposed to be “drivers” that relay requisite information for cortical functioning (Sherman and Guillery,

1996; Jones, 1998b, 2002). Thalamocortical inputs to superficial layers are proposed to be "modulators" that emerge from "matrix" neurons which span multiple thalamic nuclei, and express calbindin (CB) but not PV (Jones, 1998a; Sherman and Guillery, 1998; Guillery and Sherman, 2002). These thalamocortical inputs are thought to facilitate cortico-cortico communication and synchrony (Jones, 1998b, 2001). This pattern of input appears to be present in the monkey DLPFC (Zikopoulos and Barbas, 2007), suggesting that middle layer inputs from PV drivers and superficial inputs from CB modulators are also a convention of higher order thalamic relays to prefrontal regions. The similarities of PV-IR Type I synapses in the superficial and middle laminar zones of the human suggests, however, that quantifiable driver input from one or more thalamic nuclei is present outside of layers deep 3 – 4 of the human DLPFC. While the role of PV driver synapses in the superficial laminar zone is unclear, they may reflect axon terminals from thalamocortical relay cells that receive distinct types of inputs (Mitchell, 2015; Sherman, 2016). For example, the majority of inputs to the thalamus arise from cortical layer 6 pyramidal cells, but some relay neurons also receive glutamatergic inputs from layer 5 pyramidal cells (Guillery and Sherman, 2002; Jones, 2002; Sherman, 2016). While layer 5 inputs are the minority, they appear to be "drivers" that transmit essential information from the cortex to the thalamus. Moreover, some higher order thalamic relay neurons can receive feedback driver inputs from layer 5 pyramidal cells and/or feedforward driver inputs from subcortical structures (Groh et al., 2014; Castejon et al., 2016; Sherman, 2016). Given that layers 2 – 3 are the site of substantial cortico-cortico communication, the PV-IR thalamocortical driver inputs to these layers may provide key feedback and/or feedforward information to pyramidal cell dendrites and spines present in the superficial laminar zone of the human DLPFC.

Species-specific PFC properties and human brain disease

Despite the evolutionary relatedness of human and non-human primates, humans display species-specific, higher-order functions partially attributable to the expanded PFC (Passingham, 2009; Preuss, 2011; Smaers et al., 2011; Sherwood et al., 2012; Molnar and Pollen, 2014; Vendetti and Bunge, 2014). Indeed, the current results add to a notable literature demonstrating differences between human and multiple species of non-human primates in PFC gene and protein expression (Caceres et al., 2003; Caceres et al., 2007; Konopka et al., 2012; Muntane et al., 2015), PFC anatomy (Semendeferi et al., 2001; Raghanti et al., 2008a, b, c; Raghanti et al., 2009; Semendeferi et al., 2011; Spocter et al., 2012; Teffer et al., 2013; Raghanti et al., 2014), and PFC-mediated behaviors (reviewed in Passingham, 2009; Seed and Tomasello, 2010; Tomasello and Herrmann, 2010). For example, relative to a number of different non-human primate species, the human PFC has a protracted developmental period (reviewed in Clowry et al., 2010; Geschwind and Rakic, 2013), larger spacing between neurons (Semendeferi et al., 2011; Teffer et al., 2013), and a distinctive epigenetic methylome pattern (Farcas et al., 2009; Shulha et al., 2012; Zeng et al., 2012; Mendizabal et al., 2016). The uniqueness of the human PFC has been suggested to contribute to the apparent human specificity of certain neurodevelopmental psychiatric and neurological disorders, including autism spectrum disorder (Liu et al., 2016), schizophrenia (Ogawa and Vallender, 2014), and Alzheimer's disease (Rosen et al., 2016). Indeed, the current results inform the interpretation of disease-state postmortem human tissue findings in the DLPFC. For example, a light microscopic analysis of PV-IR varicosities (presumptive

PV axon terminals) in the superficial and middle laminar zones of the DLPFC in subjects with schizophrenia showed a significant reduction in PV-IR varicosity density selectively within the middle laminar zone (Lewis et al., 2001). Based upon monkey and rodent studies showing MD thalamic input restricted to the middle layers of the DLPFC, these results were interpreted to reflect fewer thalamic inputs, and proposed to represent one possible mechanism underlying lower dendritic spine density in this laminar location, in schizophrenia (Glantz and Lewis, 2000; Lewis et al., 2001). However, the current results add to a growing body of literature (Hashimoto et al., 2003; Dorph-Petersen et al., 2004; Glausier et al., 2014; Enwright et al., 2016) suggesting that less PV immunoreactivity in the middle laminar zone reflects a laminar-specific deficit in local PV interneurons, and not fewer thalamocortical inputs, in schizophrenia. For example, the number of neurons in the MD thalamus is not altered in schizophrenia (Cullen et al., 2003; Dorph-Petersen et al., 2004; Kreczmanski et al., 2007), and PV mRNA levels (from local PV interneurons) are lower selectively within the middle cortical layers of the DLPFC (Hashimoto et al., 2003; Chung et al., 2016). When considered with the present data that PV-IR Type I synapses are located throughout the superficial and middle layers, a more parsimonious interpretation is that fewer PV-IR varicosities in the middle layers of the DLPFC in schizophrenia likely reflects the reduction in PV protein within PV interneurons. Indeed, PV protein levels are lower in in PV somata (Enwright et al., 2016) and within local basket cell terminals in the middle layers of the DLPFC (Glausier et al., 2014).

In sum, the current data not only highlight the importance of including human brain tissue in comparative anatomical studies in order to assess how translatable findings are between species, but also provide design and interpretative value for anatomical and functional studies of human brain function in health and illness.

Acknowledgments

Support: NIMH K01MH107735 and NARSAD 23866 to JRG, NIMH 5R01MH043784 to DAL, Stanley Foundation to RCR, and 1S10RR019003-01Shared Instrument Grant. The authors thank Mary Brady for her assistance with image processing, and Dr. Susan Sesack for editorial and scientific feedback.

The authors thank Mary Brady for her assistance with image processing, and Dr. Susan Sesack for editorial and scientific feedback.

LITERATURE CITED

Amatrudo JM, Weaver CM, Crimins JL, Hof PR, Rosene DL, Luebke JI. Influence of highly distinctive structural properties on the excitability of pyramidal neurons in monkey visual and prefrontal cortices. J Neurosci. 2012; 32(40):13644–13660. [PubMed: 23035077]

Arnsten AF, Jin LE. Molecular influences on working memory circuits in dorsolateral prefrontal cortex. Progress in molecular biology and translational science. 2014; 122:211–231. [PubMed: 24484703]

Baddeley A. Working memory. Science. 1992; 255:556–559. [PubMed: 1736359]

Baimbridge KG, Celio MR, Rogers JH. Calcium-binding proteins in the nervous system. Trends in Neuroscience. 1992; 15:303–308.

Barbas H, De Olmos J. Projections from the amygdala to basoventral and prefrontal regions in the rhesus monkey. J Comp Neurol. 1990; 300:549–571. [PubMed: 2273093]

Barbas H, Haswell Henion TH, Dermon CR. Diverse thalamic projections to the prefrontal cortex in the rhesus monkey. J Comp Neurol. 1991; 313:65–94. [PubMed: 1761756]

Barch DM, Ceaser A. Cognition in schizophrenia: core psychological and neural mechanisms. Trends in cognitive sciences. 2012; 16(1):27–34. [PubMed: 22169777]

Blümcke I, Hof PR, Morrison JH, Celio MR. Distribution of parvalbumin immunoreactivity in the visual cortex of old world monkeys and humans. J Comp Neurol. 1990; 301:417–432. [PubMed: 2262599]

Blümcke I, Hof PR, Morrison JH, Celio MR. Parvalbumin in the monkey striate cortex: a quantitative immunoelectron-microscopy study. Brain Res. 1991; 554:237–243. [PubMed: 1933306]

Bordelon JR, Smith Y, Nairn AC, Colbran RJ, Greengard P, Muly EC. Differential localization of protein phosphatase-1alpha, beta and gamma1 isoforms in primate prefrontal cortex. Cereb Cortex. 2005; 15(12):1928–1937. [PubMed: 15758197]

Caceres M, Lachuer J, Zapala MA, Redmond JC, Kudo L, Geschwind DH, Lockhart DJ, Preuss TM, Barlow C. Elevated gene expression levels distinguish human from non-human primate brains. Proc Natl Acad Sci U S A. 2003; 100(22):13030–13035. [PubMed: 14557539]

Caceres M, Suwyn C, Maddox M, Thomas JW, Preuss TM. Increased cortical expression of two synaptogenic thrombospondins in human brain evolution. Cereb Cortex. 2007; 17(10):2312–2321. [PubMed: 17182969]

Castejon C, Barros-Zulaica N, Nunez A. Control of Somatosensory Cortical Processing by Thalamic Posterior Medial Nucleus: A New Role of Thalamus in Cortical Function. PLoS One. 2016; 11(1):e0148169. [PubMed: 26820514]

Celio MR. Parvalbumin in most gamma-aminobutyric acid-containing neurons of the rat cerebral cortex. Science. 1986; 231:995–998. [PubMed: 3945815]

Celio MR, Baier W, Schärer L, de Viragh PA, Gerday C. Monoclonal antibodies directed against the calcium binding protein parvalbumin. Cell Calcium. 1988; 9:81–86. [PubMed: 3383226]

Chiu CQ, Lur G, Morse TM, Carnevale NT, Ellis-Davies GC, Higley MJ. Compartmentalization of GABAergic inhibition by dendritic spines. Science. 2013; 340(6133):759–762. [PubMed: 23661763]

Chung DW, Volk DW, Arion D, Zhang Y, Sampson AR, Lewis DA. Dysregulated ErbB4 Splicing in Schizophrenia: Selective Effects on Parvalbumin Expression. Am J Psychiatry. 2016; 173(1):60–68. [PubMed: 26337038]

Clowry G, Molnar Z, Rakic P. Renewed focus on the developing human neocortex. J Anat. 2010; 217(4):276–288. [PubMed: 20979582]

Conde F, Lund JS, Jacobowitz DM, Baimbridge KG, Lewis DA. Local circuit neurons immunoreactive for calretinin, calbindin D-28k or parvalbumin in monkey prefrontal cortex: distribution and morphology. J Comp Neurol. 1994; 341(1):95–116. [PubMed: 8006226]

Constantinidis C, Procyk E. The primate working memory networks. Cogn Affect Behav Neurosci. 2004; 4(4):444–465. [PubMed: 15849890]

Cullen TJ, Walker MA, Parkinson N, Craven R, Crow TJ, Esiri MM, Harrison PJ. A postmortem study of the mediodorsal nucleus of the thalamus in schizophrenia. Schizophr Res. 2003; 60:157–166. [PubMed: 12591579]

DeFelipe J. Types of neurons, synaptic connections and chemical characteristics of cells immunoreactive for calbindin-D28K, parvalbumin and calretinin in the neocortex. Journal of Chemical Neuroanatomy. 1997; 14:1–19. [PubMed: 9498163]

DeFelipe J, Alonso-Nanclares L, Arellano JI. Microstructure of the neocortex: comparative aspects. J Neurocytol. 2002; 31(3–5):299–316. [PubMed: 12815249]

DeFelipe J, Farinas I. The pyramidal neuron of the cerebral cortex: Morphological and chemical characteristics of the synaptic inputs. Progress in Neurobiology. 1992; 39:563–607. [PubMed: 1410442]

DeFelipe J, Jones EG. Parvalbumin immunoreactivity reveals layer IV of monkey cerebral cortex as a mosaic of microzones of thalamic afferent terminations. Brain Res. 1991; 562:39–47. [PubMed: 1799871]

del Río MR, DeFelipe J. A study of SMI 32-stained pyramidal cells, parvalbumin-immunoreactive chandelier cells, and presumptive thalamorcortical axons in the human temporal neocortex. J Comp Neurol. 1994; 342:389–408. [PubMed: 7517410]

Dorph-Petersen KA, Pierri JN, Sun Z, Sampson AR, Lewis DA. Stereological analysis of the mediodorsal thalamic nucleus in schizophrenia: Volume, neuron number, and cell types. J Comp Neurol. 2004; 472(4):449–462. [PubMed: 15065119]

Elston GN. Cortex, cognition and the cell: new insights into the pyramidal neuron and prefrontal function. Cereb Cortex. 2003; 13(11):1124–1138. [PubMed: 14576205]

Enwright JF, Sanapala S, Foglio A, Berry R, Fish KN, Lewis DA. Reduced Labeling of Parvalbumin Neurons and Perineuronal Nets in the Dorsolateral Prefrontal Cortex of Subjects with Schizophrenia. Neuropsychopharmacology. 2016

Erickson SL, Lewis DA. Cortical connections of the lateral mediodorsal thalamus in cynomolgus monkeys. J Comp Neurol. 2004; 473:107–127. [PubMed: 15067722]

Familtsev D, Quiggins R, Masterson SP, Dang W, Slusarczyk AS, Petry HM, Bickford ME. Ultrastructure of geniculocortical synaptic connections in the tree shrew striate cortex. J Comp Neurol. 2016; 524(6):1292–1306. [PubMed: 26399201]

Farcas R, Schneider E, Frauenknecht K, Kondova I, Bontrop R, Bohl J, Navarro B, Metzler M, Zischler H, Zechner U, Daser A, Haaf T. Differences in DNA methylation patterns and expression of the CCRK gene in human and nonhuman primate cortices. Molecular biology and evolution. 2009; 26(6):1379–1389. [PubMed: 19282513]

Fitzgerald ML, Chan J, Mackie K, Lupica CR, Pickel VM. Altered dendritic distribution of dopamine D2 receptors and reduction in mitochondrial number in parvalbumin-containing interneurons in the medial prefrontal cortex of cannabinoid-1 (CB1) receptor knockout mice. J Comp Neurol. 2012; 520(17):4013–4031. [PubMed: 22592925]

Freund TF, Martin KA, Whitteridge D. Innervation of cat visual areas 17 and 18 by physiologically identified X- and Y- type thalamic afferents. I. Arborization patterns and quantitative distribution of postsynaptic elements. J Comp Neurol. 1985; 242(2):263–274. [PubMed: 4086666]

Freund TF, Martin KAC, Soltescz I, Somogyi P, Whitteridge D. Arborization pattern and postsynaptic targets of physiologically identified thalamocortical afferents in striate cortex of the macaque monkey. J Comp Neurol. 1989; 289:315–336. [PubMed: 2808770]

Gabbott PL, Bacon SJ. Local circuit neurons in the medial prefrontal cortex (areas 24a,b,c, 25 and 32) in the monkey: I. Cell morphology and morphometrics. J Comp Neurol. 1996; 364(4):567–608. [PubMed: 8821449]

Garcia-Marin V, Ahmed TH, Afzal YC, Hawken MJ. Distribution of vesicular glutamate transporter 2 (VGluT2) in the primary visual cortex of the macaque and human. J Comp Neurol. 2013; 521(1): 130–151. [PubMed: 22684983]

Germano C, Kinsella GJ. Working memory and learning in early Alzheimer's disease. Neuropsychol Rev. 2005; 15(1):1–10. [PubMed: 15929495]

Geschwind DH, Rakic P. Cortical evolution: judge the brain by its cover. Neuron. 2013; 80(3):633–647. [PubMed: 24183016]

Giguere M, Goldman-Rakic PS. Mediodorsal nucleus: Areal, laminar, and tangential distribution of afferents and efferents in the frontal lobe of rhesus monkeys. J Comp Neurol. 1988; 277:195–213. [PubMed: 2466057]

Gil Z, Connors BW, Amitai Y. Efficacy of thalamocortical and intracortical synaptic connections: quanta, innervation, and reliability. Neuron. 1999; 23(2):385–397. [PubMed: 10399943]

Glantz LA, Lewis DA. Decreased dendritic spine density on prefrontal cortical pyramidal neurons in schizophrenia. Arch Gen Psychiatry. 2000; 57:65–73. [PubMed: 10632234]

Glausier JR, Fish KN, Lewis DA. Altered parvalbumin basket cell inputs in the dorsolateral prefrontal cortex of schizophrenia subjects. Mol Psychiatry. 2014; 19(1):30–36. [PubMed: 24217255]

Glausier JR, Khan ZU, Muly EC. Dopamine D1 and D5 receptors are localized to discrete populations of interneurons in primate prefrontal cortex. Cereb Cortex. 2009; 19(8):1820–1834. [PubMed: 19020206]

Goldman-Rakic PS, Porrino LJ. The primate mediodorsal (MD) nucleus and its projection to the frontal lobe. J Comp Neurol. 1985; 242:535–560. [PubMed: 2418080]

Groh A, Bokor H, Mease RA, Plattner VM, Hangya B, Stroh A, Deschenes M, Acsady L. Convergence of cortical and sensory driver inputs on single thalamocortical cells. Cereb Cortex. 2014; 24(12):3167–3179. [PubMed: 23825316]

Guillery RW, Sherman SM. Thalamic relay functions and their role in corticocortical communication: Generalizations from the visual system. Neuron. 2002; 33:163–175. [PubMed: 11804565]

Gulyas AI, Buzsaki G, Freund TF, Hirase H. Populations of hippocampal inhibitory neurons express different levels of cytochrome c. Eur J Neurosci. 2006; 23(10):2581–2594. [PubMed: 16817861]

Gutierrez C, Cola MG, Seltzer B, Cusik C. Neurochemical and connectional organization of the dorsal pulvinar complex in monkeys. J Comp Neurol. 2000; 419:61–86. [PubMed: 10717640]

Hackney CM, Mahendrasingam S, Penn A, Fettiplace R. The concentrations of calcium buffering proteins in mammalian cochlear hair cells. J Neurosci. 2005; 25(34):7867–7875. [PubMed: 16120789]

Hashimoto T, Volk DW, Eggan SM, Mirnics K, Pierri JN, Sun Z, Sampson AR, Lewis DA. Gene expression deficits in a subclass of GABA neurons in the prefrontal cortex of subjects with schizophrenia. J Neurosci. 2003; 23:6315–6326. [PubMed: 12867516]

Hendry SHC, Schwark HD, Jones EG, Yan J. Numbers and proportions of GABA-immunoreactive neurons in different areas of monkey cerebral cortex. J Neurosci. 1987; 7:1503–1519. [PubMed: 3033170]

Hof PR, Bogaert YE, Rosenthal RE, Fiskum G. Distribution of neuronal populations containing neurofilament protein and calcium-binding proteins in the canine neocortex: regional analysis and cell typology. J Chem Neuroanat. 1996a; 11(2):81–98. [PubMed: 8877597]

Hof PR, Cox K, Young WG, Celio MR, Rogers J, Morrison JH. Parvalbumin-immunoreactive neurons in the neocortex are resistant to degeneration in Alzheimer's disease. J Neuropathol Exp Neurol. 1991; 50:451–462. [PubMed: 2061713]

Hof PR, Glezer II, Conde F, Flagg RA, Rubin MB, Nimchinsky EA, Vogt Weisenhorn DM. Cellular distribution of the calcium-binding proteins parvalbumin, calbindin, and calretinin in the neocortex of mammals: phylogenetic and developmental patterns. J Chem Neuroanat. 1999; 16(2):77–116. [PubMed: 10223310]

Hof PR, Rosenthal RE, Fiskum G. Distribution of neurofilament protein and calcium-binding proteins parvalbumin, calbindin, and calretinin in the canine hippocampus. J Chem Neuroanat. 1996b; 11(1):1–12. [PubMed: 8841885]

Hornung JP, DeTribolet N. Distribution of GABA-containing neurons in human frontal cortex: A quantitative immunocytochemical study. AnatEmbryol. 1994; 189:139–145.

Ichinohe N, Watakabe A, Miyashita T, Yamamori T, Hashikawa T, Rockland KS. A voltage-gated potassium channel, Kv3.1b, is expressed by a subpopulation of large pyramidal neurons in layer 5 of the macaque monkey cortex. Neuroscience. 2004; 129(1):179–185. [PubMed: 15489040]

Jahn H. Memory loss in Alzheimer's disease. Dialogues in clinical neuroscience. 2013; 15(4):445–454. [PubMed: 24459411]

Jones EG. A new view of specific and nonspecific thalamocortical connections. Adv Neurol. 1998a; 77:49–71. discussion 72–43. [PubMed: 9709817]

Jones EG. Viewpoint: The core and matrix of thalamic organization. Neuroscience. 1998b; 85:331–345. [PubMed: 9622234]

Jones EG. The thalamic matrix and thalamocortical synchrony. Trends Neurosci. 2001; 24(10):595–601. [PubMed: 11576674]

Jones EG. Thalamic circuitry and thalamocortical synchrony. Philosophical transactions of the Royal Society of London Series B, Biological sciences. 2002; 357(1428):1659–1673. [PubMed: 12626002]

Jones EG, Hendry SHC. Differential calcium binding protein immunoreactivity distinguishes classes of relay neurons in monkey thalamic nuclei. European Journal of Neuroscience. 1989; 1:222–246. [PubMed: 12106154]

Kann O, Papageorgiou IE, Draguhn A. Highly energized inhibitory interneurons are a central element for information processing in cortical networks. J Cereb Blood Flow Metab. 2014; 34(8):1270–1282. [PubMed: 24896567]

Kievit J, Kuypers HGJM. Organization of the thalamo-cortical connections to the frontal lobe in the rhesus monkey. Exp Brain Res. 1977; 29:299–322. [PubMed: 410652]

Konopka G, Friedrich T, Davis-Turak J, Winden K, Oldham MC, Gao F, Chen L, Wang GZ, Luo R, Preuss TM, Geschwind DH. Human-specific transcriptional networks in the brain. Neuron. 2012; 75(4):601–617. [PubMed: 22920253]

Kreczmanski P, Heinsen H, Mantua V, Woltersdorf F, Masson T, Ulfig N, Schmidt-Kastner R, Korr H, Steinbusch HWM, Hof PR, Schmitz C. Volume, neuron density and total neuron number in five subcortical regions in schizophrenia. Brain. 2007; 130(Pt 3):678–692. [PubMed: 17303593]

Kubota Y, Karube F, Nomura M, Kawaguchi Y. The Diversity of Cortical Inhibitory Synapses. Frontiers in neural circuits. 2016; 10:27. [PubMed: 27199670]

Kubota Y, Kondo S, Nomura M, Hatada S, Yamaguchi N, Mohamed AA, Karube F, Lubke J, Kawaguchi Y. Functional effects of distinct innervation styles of pyramidal cells by fast spiking cortical interneurons. eLife. 2015:4.

Lewis DA, Cruz DA, Melchitzky DS, Pierri JN. Lamina-specific deficits in parvalbumin-immunoreactive varicosities in the prefrontal cortex of subjects with schizophrenia: Evidence for fewer projections from the thalamus. Am J Psychiatry. 2001; 158:1411–1422. [PubMed: 11532725]

Lewis DA, Curley AA, Glausier JR, Volk DW. Cortical parvalbumin interneurons and cognitive dysfunction in schizophrenia. Trends Neurosci. 2012; 35(1):57–67. [PubMed: 22154068]

Liu X, Han D, Somel M, Jiang X, Hu H, Guijarro P, Zhang N, Mitchell A, Halene T, Ely JJ, Sherwood CC, Hof PR, Qiu Z, Paabo S, Akbarian S, Khaitovich P. Disruption of an Evolutionarily Novel Synaptic Expression Pattern in Autism. PLoS Biol. 2016; 14(9):e1002558. [PubMed: 27685936]

Lund JS, Lewis DA. Local circuit neurons of developing and mature macaque prefrontal cortex: Golgi and immunocytochemical characteristics. J Comp Neurol. 1993; 328:282–312. [PubMed: 7678612]

Mascagni F, Muly EC, Rainnie DG, McDonald AJ. Immunohistochemical characterization of parvalbumin-containing interneurons in the monkey basolateral amygdala. Neuroscience. 2009; 158(4):1541–1550. [PubMed: 19059310]

McFarland NR, Haber SN. Thalamic relay nuclei of the basal ganglia form both reciprocal and nonreciprocal cortical connections, linking multiple frontal cortical areas. J Neurosci. 2002; 22:8117–8132. [PubMed: 12223566]

Medalla M, Luebke JI. Diversity of glutamatergic synaptic strength in lateral prefrontal versus primary visual cortices in the rhesus monkey. J Neurosci. 2015; 35(1):112–127. [PubMed: 25568107]

Melchitzky DS, Sesack SR, Lewis DA. Parvalbumin-immunoreactive axon terminals in macaque monkey and human prefrontal cortex: Laminar, regional and target specificity of Type I and Type II synapses. J Comp Neurol. 1999; 408:11–22. [PubMed: 10331577]

Mendizabal I, Shi L, Keller TE, Konopka G, Preuss TM, Hsieh TF, Hu E, Zhang Z, Su B, Yi SV. Comparative Methylome Analyses Identify Epigenetic Regulatory Loci of Human Brain Evolution. Molecular biology and evolution. 2016; 33(11):2947–2959. [PubMed: 27563052]

Mitchell AS. The mediodorsal thalamus as a higher order thalamic relay nucleus important for learning and decision-making. Neurosci Biobehav Rev. 2015; 54:76–88. [PubMed: 25757689]

Miyashita T, Ichinohe N, Rockland KS. Differential modes of termination of amygdalothalamic and amygdalocortical projections in the monkey. J Comp Neurol. 2007; 502(2):309–324. [PubMed: 17348015]

Molinari M, Dell'Anna ME, Rausell E, Leggio MG, Hashikawa T, Jones EG. Auditory thalamocortical pathways defined in monkeys by calcium-binding protein immunoreactivity. J Comp Neurol. 1995; 362:171–194. [PubMed: 8576432]

Molnar Z, Pollen A. How unique is the human neocortex? Development. 2014; 141(1):11–16. [PubMed: 24346696]

Munkle MC, Waldvogel HJ, Faull RLM. Calcium-binding protein immunoreactivity delineates the intralaminar nuclei of the thalamus in the human brain. Neuroscience. 1999; 90:485–491. [PubMed: 10215153]

Muntane G, Horvath JE, Hof PR, Ely JJ, Hopkins WD, Raghanti MA, Lewandowski AH, Wray GA, Sherwood CC. Analysis of synaptic gene expression in the neocortex of primates reveals evolutionary changes in glutamatergic neurotransmission. Cereb Cortex. 2015; 25(6):1596–1607. [PubMed: 24408959]

Negyessy L, Goldman-Rakic PS. Morphometric characterization of synapses in the primate prefrontal cortex formed by afferents from the mediodorsal thalamic nucleus. Exp Brain Res. 2005; 164(2): 148–154. [PubMed: 15776222]

O'Hearn K, Asato M, Ordaz S, Luna B. Neurodevelopment and executive function in autism. Dev Psychopathol. 2008; 20(4):1103–1132. [PubMed: 18838033]

Ogawa LM, Vallender EJ. Evolutionary conservation in genes underlying human psychiatric disorders. Front Hum Neurosci. 2014; 8:283. [PubMed: 24834046]

Park HS, Park SJ, Park SH, Chun MH, Oh SJ. Shifting of parvalbumin expression in the rat retina in experimentally induced diabetes. Acta Neuropathol. 2008; 115(2):241–248. [PubMed: 17989985]

Passingham, R. What is Special About the Human Brain?. Oxford, England: Oxford University Press; 2008.

Passingham R. How good is the macaque monkey model of the human brain? Curr Opin Neurobiol. 2009; 19(1):6–11. [PubMed: 19261463]

Peters, A., Palay, SL., Webster, DF. The Fine Structure of The Nervous System. New York: Oxford University Press; 1991.

Petrides M. Lateral prefrontal cortex: architectonic and functional organization. Philosophical transactions of the Royal Society of London Series B, Biological sciences. 2005; 360(1456):781–795. [PubMed: 15937012]

Pirot S, Jay TM, Glowinski J, Thierry AM. Anatomical and electrophysiological evidence for an excitatory amino acid pathway from the thalamic mediodorsal nucleus to the prefrontal cortex in the rat. European Journal of Neuroscience. 1994; 6:1225–1234. [PubMed: 7524967]

Preuss TM. The human brain: rewired and running hot. Ann N Y Acad Sci. 2011; 1225(Suppl 1):E182–191. [PubMed: 21599696]

Preuss TM, Coleman GQ. Human-specific organization of primary visual cortex: alternating compartments of dense Cat-301 and calbindin immunoreactivity in layer 4A. Cereb Cortex. 2002; 12(7):671–691. [PubMed: 12050080]

Preuss TM, Kaas JH. Parvalbumin-like immunoreactivity of layer V pyramidal cells in the motor and somatosensory cortex of adult primates. Brain Res. 1996; 712:353–357. [PubMed: 8814914]

Preuss TM, Qi H, Kaas JH. Distinctive compartmental organization of human primary visual cortex. Proc Natl Acad Sci U S A. 1999; 96(20):11601–11606. [PubMed: 10500223]

Raghanti MA, Edler MK, Meindl RS, Sudduth J, Bohush T, Erwin JM, Stimpson CD, Hof PR, Sherwood CC. Humans and great apes share increased neocortical neuropeptide Y innervation compared to other haplorhine primates. Front Hum Neurosci. 2014; 8:101. [PubMed: 24616688]

Raghanti MA, Spocter MA, Stimpson CD, Erwin JM, Bonar CJ, Allman JM, Hof PR, Sherwood CC. Species-specific distributions of tyrosine hydroxylase-immunoreactive neurons in the prefrontal cortex of anthropoid primates. Neuroscience. 2009; 158(4):1551–1559. [PubMed: 19041377]

Raghanti MA, Stimpson CD, Marcinkiewicz JL, Erwin JM, Hof PR, Sherwood CC. Cholinergic innervation of the frontal cortex: differences among humans, chimpanzees, and macaque monkeys. J Comp Neurol. 2008a; 506(3):409–424. [PubMed: 18041783]

Raghanti MA, Stimpson CD, Marcinkiewicz JL, Erwin JM, Hof PR, Sherwood CC. Cortical dopaminergic innervation among humans, chimpanzees, and macaque monkeys: a comparative study. Neuroscience. 2008b; 155(1):203–220. [PubMed: 18562124]

Raghanti MA, Stimpson CD, Marcinkiewicz JL, Erwin JM, Hof PR, Sherwood CC. Differences in cortical serotonergic innervation among humans, chimpanzees, and macaque monkeys: a comparative study. Cereb Cortex. 2008c; 18(3):584–597. [PubMed: 17586605]

Roberts RC, Xu L, Roche JK, Kirkpatrick B. Ultrastructural localization of reelin in the cortex in post-mortem human brain. J Comp Neurol. 2005; 482(3):294–308. [PubMed: 15690491]

Romanski LM, Giguere M, Bates JF, Goldman-Rakic PS. Topographic organization of medial pulvinar connections with the prefrontal cortex in the rhesus monkey. J Comp Neurol. 1997; 379:313–332. [PubMed: 9067827]

Rosen RF, Tomidokoro Y, Farberg AS, Dooyema J, Ciliax B, Preuss TM, Neubert TA, Ghiso JA, LeVine H 3rd, Walker LC. Comparative pathobiology of beta-amyloid and the unique susceptibility of humans to Alzheimer's disease. Neurobiol Aging. 2016; 44:185–196. [PubMed: 27318146]

Rotaru DC, Barrionuevo G, Sesack SR. Mediodorsal thalamic afferents to layer III of the rat prefrontal cortex: synaptic relationships to subclasses of interneurons. J Comp Neurol. 2005; 490(3):220–238. [PubMed: 16082676]

Schoonover CE, Tapia JC, Schilling VC, Wimmer V, Blazeski R, Zhang W, Mason CA, Bruno RM. Comparative strength and dendritic organization of thalamocortical and corticocortical synapses onto excitatory layer 4 neurons. J Neurosci. 2014; 34(20):6746–6758. [PubMed: 24828630]

Schwaller B, Dick J, Dhoot G, Carroll S, Vrbova G, Nicotera P, Pette D, Wyss A, Bluethmann H, Hunziker W, Celio MR. Prolonged contraction-relaxation cycle of fast-twitch muscles in parvalbumin knockout mice. Am J Physiol. 1999; 276(2 Pt 1):C395–C403. [PubMed: 9950767]

Seed A, Tomasello M. Primate cognition. Topics in cognitive science. 2010; 2(3):407–419. [PubMed: 25163869]

Semendeferi K, Armstrong E, Schleicher A, Zilles K, Van Hoesen GW. Prefrontal cortex in humans and apes: a comparative study of area 10. American journal of physical anthropology. 2001; 114(3):224–241. [PubMed: 11241188]

Semendeferi K, Teffer K, Buxhoeveden DP, Park MS, Bludau S, Amunts K, Travis K, Buckwalter J. Spatial organization of neurons in the frontal pole sets humans apart from great apes. Cereb Cortex. 2011; 21(7):1485–1497. [PubMed: 21098620]

Sherman SM. Thalamus plays a central role in ongoing cortical functioning. Nat Neurosci. 2016; 16(4):533–541.

Sherman SM, Guillery RW. Functional organization of thalamocortical relays. J Neurophysiol. 1996; 76:1367–1395. [PubMed: 8890259]

Sherman SM, Guillery RW. On the actions that one nerve cell can have another: Distinguishing “drivers” from “modulators”. Proceedings of the National Academy of Sciences USA. 1998; 95:7121–7126.

Sherwood CC, Bauernfeind AL, Bianchi S, Raghanti MA, Hof PR. Human brain evolution writ large and small. Prog Brain Res. 2012; 195:237–254. [PubMed: 22230630]

Sherwood CC, Stimpson CD, Butti C, Bonar CJ, Newton AL, Allman JM, Hof PR. Neocortical neuron types in Xenarthra and Afrotheria: implications for brain evolution in mammals. Brain structure & function. 2009; 213(3):301–328. [PubMed: 19011898]

Shulha HP, Crisci JL, Reshetov D, Tushir JS, Cheung I, Bharadwaj R, Chou HJ, Houston IB, Peter CJ, Mitchell AC, Yao WD, Myers RH, Chen JF, Preuss TM, Rogaev EI, Jensen JD, Weng Z, Akbarian S. Human-specific histone methylation signatures at transcription start sites in prefrontal neurons. PLoS Biol. 2012; 10(11):e1001427. [PubMed: 23185133]

Silbereis JC, Pochareddy S, Zhu Y, Li M, Sestan N. The Cellular and Molecular Landscapes of the Developing Human Central Nervous System. Neuron. 2016; 89(2):248–268. [PubMed: 26796689]

Smaers JB, Steele J, Case CR, Cowper A, Amunts K, Zilles K. Primate prefrontal cortex evolution: human brains are the extreme of a lateralized ape trend. Brain Behav Evol. 2011; 77(2):67–78. [PubMed: 21335939]

Sorvari H, Soininen H, Paljärvi L, Karkola K, Pitkänen A. Distribution of parvalbumin-immunoreactive cells and fibers in the human amygdaloid complex. J Comp Neurol. 1995; 360:185–212. [PubMed: 8522643]

Spocter MA, Hopkins WD, Barks SK, Bianchi S, Hehmeyer AE, Anderson SM, Stimpson CD, Fobbs AJ, Hof PR, Sherwood CC. Neuropil distribution in the cerebral cortex differs between humans and chimpanzees. J Comp Neurol. 2012; 520(13):2917–2929. [PubMed: 22350926]

Takacs VT, Szonyi A, Freund TF, Nyiri G, Gulyas AI. Quantitative ultrastructural analysis of basket and axo-axonic cell terminals in the mouse hippocampus. Brain structure & function. 2015; 220(2):919–940. [PubMed: 24407853]

Teffer K, Buxhoeveden DP, Stimpson CD, Fobbs AJ, Schapiro SJ, Baze WB, McArthur MJ, Hopkins WD, Hof PR, Sherwood CC, Semendeferi K. Developmental changes in the spatial organization of neurons in the neocortex of humans and common chimpanzees. J Comp Neurol. 2013; 521(18):4249–4259. [PubMed: 23839595]

Tomasello M, Herrmann E. Ape and Human Cognition: What’s the Difference? Current Directions in Psychological Science. 2010; 19(1):3–8.

Vendetti MS, Bunge SA. Evolutionary and developmental changes in the lateral frontoparietal network: a little goes a long way for higher-level cognition. Neuron. 2014; 84(5):906–917. [PubMed: 25475185]

Volk DW, Radchenkova PV, Walker EM, Sengupta EJ, Lewis DA. Cortical opioid markers in schizophrenia and across postnatal development. Cereb Cortex. 2012; 22(5):1215–1223. [PubMed: 21810780]

Watanabe Y, Funahashi S. Thalamic mediodorsal nucleus and working memory. Neurosci Biobehav Rev. 2012; 36(1):134–142. [PubMed: 21605592]

White, EL. Termination of thalamic afferents in the cerebral cortex. In: Jones, EG., Peters, A., editors. Cereb Cortex. Vol. 5. New York: Plenum Press; 1986. p. 271-285.

Williams SM, Goldman-Rakic PS, Leranth C. The synaptology of parvalbumin-immunoreactive neurons in primate prefrontal cortex. J Comp Neurol. 1992; 320:353–369. [PubMed: 1613130]

Woo TU, Miller JL, Lewis DA. Schizophrenia and the parvalbumin-containing class of cortical local circuit neurons. Am J Psychiatry. 1997; 154(7):1013–1015. [PubMed: 9210755]

Zeng J, Konopka G, Hunt BG, Preuss TM, Geschwind D, Yi SV. Divergent whole-genome methylation maps of human and chimpanzee brains reveal epigenetic basis of human regulatory evolution. Am J Hum Genet. 2012; 91(3):455–465. [PubMed: 22922032]

Zikopoulos B, Barbas H. Parallel driving and modulatory pathways link the prefrontal cortex and thalamus. PLoS One. 2007; 2(9):e848. [PubMed: 17786219]

Zikopoulos B, Barbas H. Altered neural connectivity in excitatory and inhibitory cortical circuits in autism. Front Hum Neurosci. 2013; 7:609. [PubMed: 24098278]

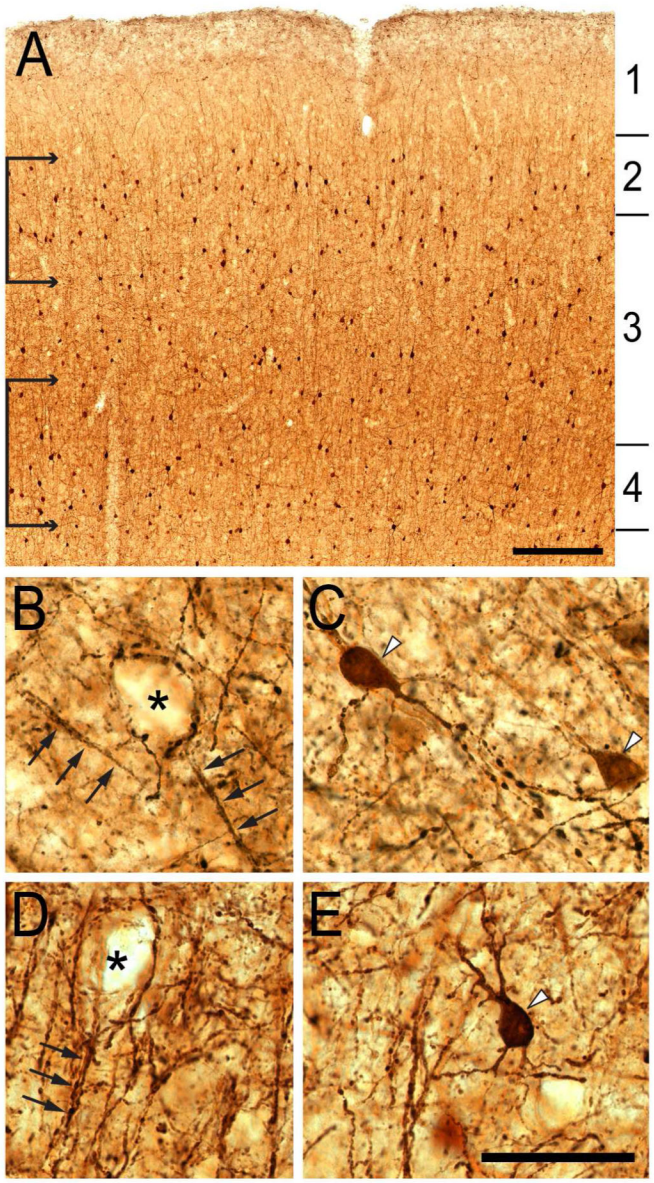

Figure 1. Light micrographs of PV labeling in human DLPFC area 9

A: Representative PV labeling in layers 1 – 4. Brackets indicate the sampling regions for the superficial (layers 2 – superficial 3) and middle (layers deep 3 – 4) laminar zones. **B:** PV-IR basket (asterisk) and cartridge (arrows) formations in the superficial laminar zone. These inputs are characteristic of GABAergic basket and chandelier cells, respectively. **C:** PV-IR somata (arrowheads) in the superficial laminar zone. Note multiple punctated processes, some of which appear to be beaded dendrites and others may be varicose axons. **D:** PV-IR basket (asterisk) and cartridge (arrows) formations in the middle laminar zone. **E:** A PV-IR soma (arrowhead) in the middle laminar zone. In B-E, PV-IR puncta from unknown sources, in addition to those characteristic of interneurons, are prevalent throughout the neuropil. Scale bar is 300 μm for A, and 50 μm for B–E.

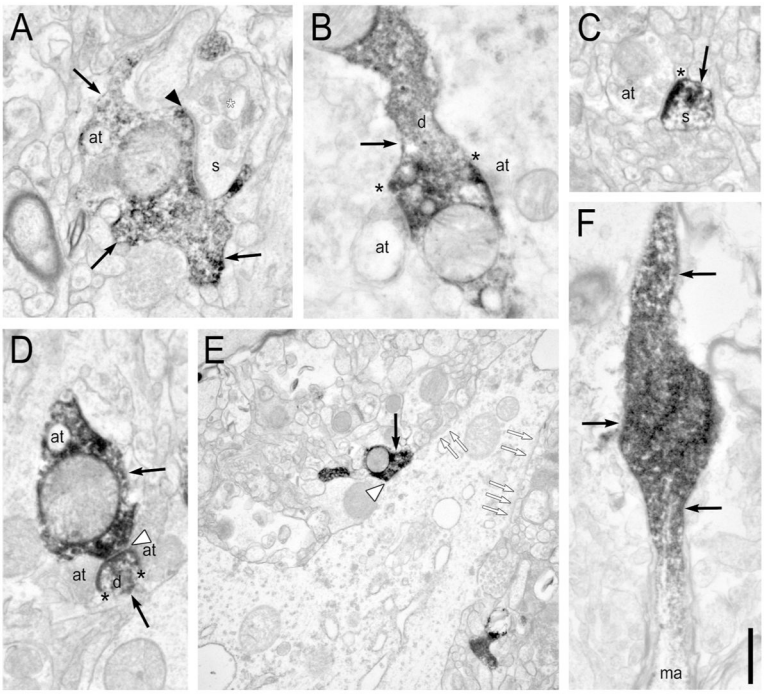

Figure 2. Electron micrographs of PV labeling in human DLPFC area 9

A: PV-IR axon terminal (arrows) forming a Type I synapse (black arrowhead) with a large dendritic spine. Note the extensive spine apparatus (white asterisk). **B:** A PV-IR dendritic shaft (arrow) receiving two Type I synapses (black asterisks) from non-PV-IR, presumably glutamatergic, axon terminals. **C:** A rarely identified PV-IR dendritic spine (arrow) receiving a Type I synapse (black asterisk) from a non-PV-IR, presumably glutamatergic, axon terminal. **D:** A PV-IR axon terminal (top arrow) forming a Type II synapse (white arrowhead) with a small PV-IR dendritic profile (bottom arrow). The dendrite is also receiving two Type I synapses (asterisks) from non-PV-IR, presumably glutamatergic, axon terminals. Subsequent serial sections confirm these two Type I synapses are from two distinct axon terminals. **E:** A PV-IR axon terminal (black arrow) forming a Type II synapse (white arrowhead) with an axon initial segment. Note the dense undercoating in the axon initial segment (white arrows). **F:** A PV-IR *en passant* terminal (arrows). Note the myelin that surrounds the axon is absent around the terminal swelling, and the PV labeling is largely restricted to the terminal and proximal axon. Myelinated e*n passant* axons are characteristic of inputs to DLPFC middle layers from the mediodorsal thalamus (Erickson and Lewis, 2004). at- axon terminal, d- dendrite, s- spine. at- axon terminal, d- dendrite, ma- myelinated axon, s- spine. Scale bar is 500 nm for A-D and F, 975 nm for E, and 715 nm for F.

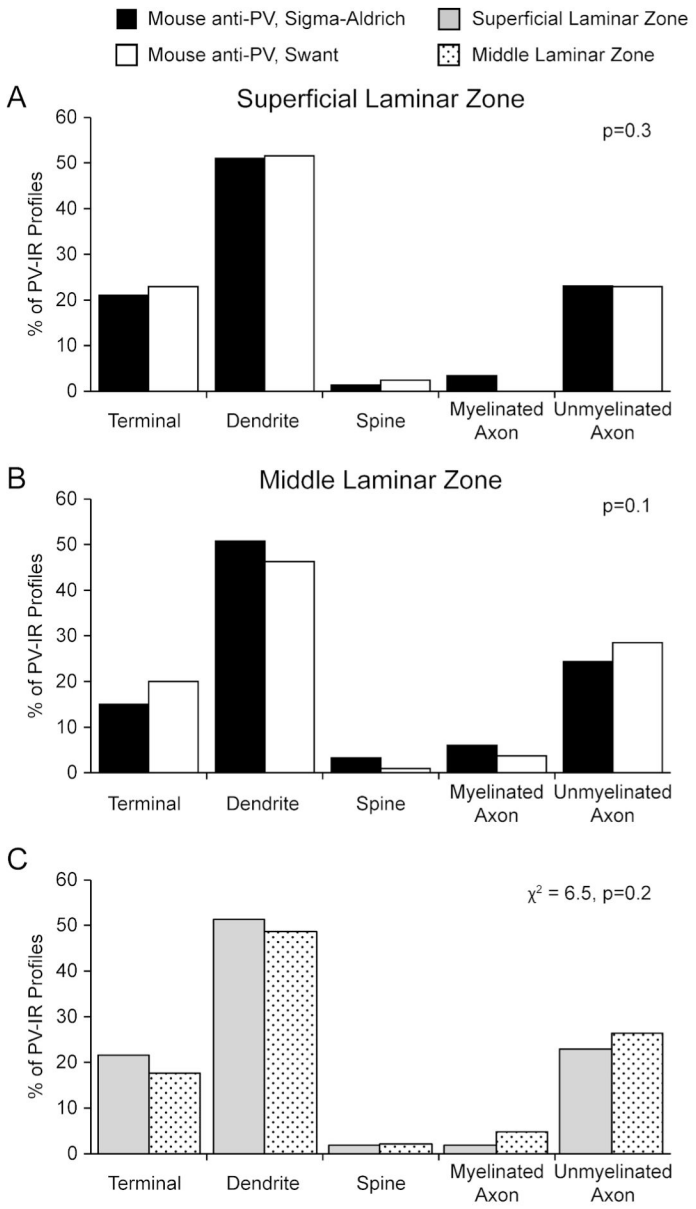

Figure 3. Histograms showing the relative distribution of PV immunoreactivity across the neuropil

A: Distribution of PV immunoreactivity in the superficial laminar zone as revealed by two different PV antibodies. The distribution of PV-IR profiles does not differ between antibodies (p=0.3). **B:** Distribution of PV immunoreactivity in the superficial laminar zone as revealed by two different PV antibodies. The distribution of PV-IR profiles does not differ between antibodies (p=0.1). **C:** The distribution of PV-IR profiles from both antibodies was combined within a laminar zone. The types of neuronal profiles labeled for PV does not significantly differ between laminar zones ($\chi^2 = 6.5$, p =0.2).

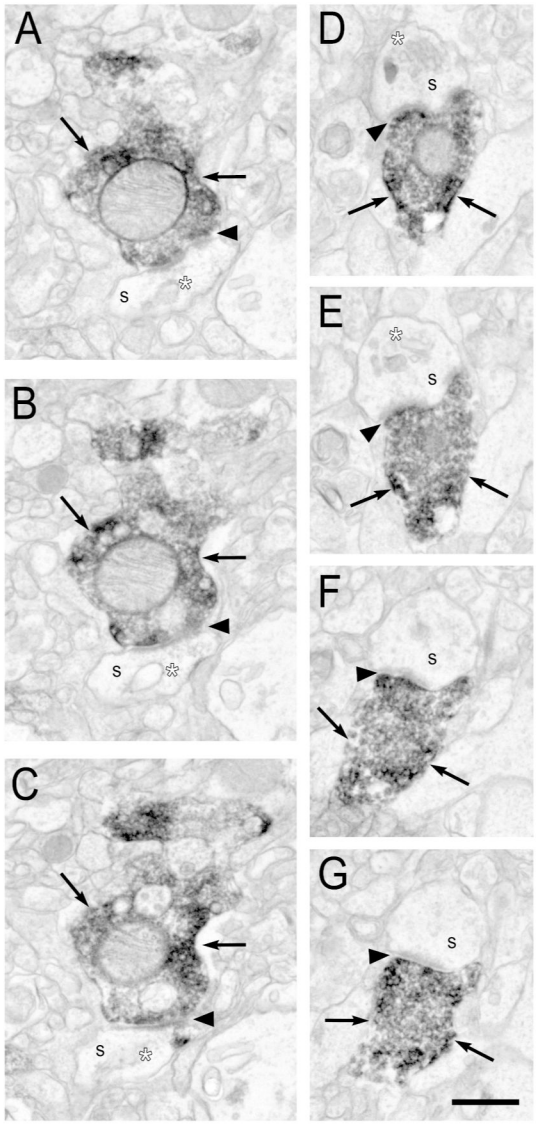

Figure 4. Serial sections of electron micrographs illustrating Type I PV synapses

A–C: A PV-IR axon terminal (arrows) in the superficial laminar zone forming a Type I synapse (black arrowhead) with an unlabeled dendritic spine that contains a spine apparatus (white asterisk). **D–G:** A PV-IR axon terminal (arrows) in the middle laminar zone forming a perforated Type I synapse (black arrowhead) with an unlabeled dendritic spine. Note the presence of a spine apparatus (white asterisk) in D–E. s- spine. Scale bar is 500 nm.

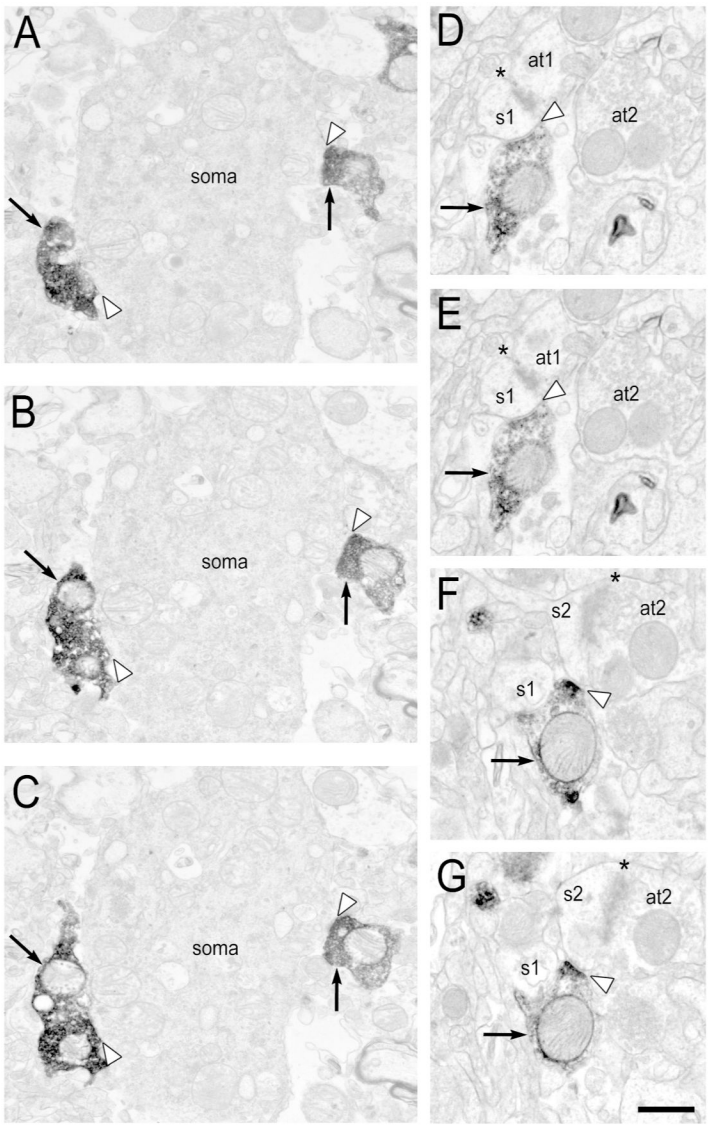

Figure 5. Serial sections of electron micrographs illustrating Type II PV synapses

A–C: Two PV-IR axon terminals (arrows) in the superficial laminar zone forming Type II synapses (white arrowheads) with an unlabeled soma or very proximal dendrite. **D–G:** A PV-IR axon

Table 1

Human Subject Characteristics

Subject	Tissue Source	Age	Sex	Race	PMI
554	MBC	32	F	W	7.0
580	MBC	43	F	B	6.0
344	Pitt	50	M	W	6.8
727	Pitt	19	M	B	7.0

MBC: Maryland Brain Collection; Pitt: University of Pittsburgh; PMI: postmortem interval (hr)

Table 2

Primary Antibodies Used

Antigen	Immunogen	Manufacturer	RRID	Species	Concentration
Parvalbumin	Frog muscle	Sigma-Aldrich, #P3088	AB_477329	Mouse, monoclonal	1:10,000
Parvalbumin	Carp muscle	Swant, #235	AB_10000343	Mouse, monoclonal	1:5,000

Table 3

Comparison of Type I and Type II PV Synapses in the Superficial and Middle Laminar Zones

Laminar Zone	Synapse Type	% of PV Synapses	% of All Type I Synapses
Superficial	Type I	44% (n=21 of 48)	2.5% (n=21 of 829)
	Type II	56% (n=27 of 48)	--
Middle	Type I	39% (n=23 of 59)	3.1% (n=23 of 747)
	Type II	61% (n=36 of 59)	--

Table 4

Comparison of Postsynaptic Targets of PV Synapses in the Superficial and Middle Laminar Zones

Laminar Zone	Synapse Type	Postsynaptic Target					
		Spine	Dendrite	PV Dendrite	Soma	AIS	Unknown
Superficial	Type I	100%	--	--	--	--	--
	Type II	30%	48%	--	18%	--	4%
Middle	Type I	52%	35%	13%	--	--	--
	Type II	14%	50%	3%	19%	11%	3%

Table 5

Comparison of Mitochondria Prevalence in PV-IR Axonal Boutons

	Superficial Laminar Zone # of Mitochondria/Bouton					Middle Laminar Zone # of Mitochondria/Bouton				
	0	**1**	**2**	**3**	**>3**	**0**	**1**	**2**	**3**	**>3**
All PV Boutons	24%	58%	15%	2%	1%	27%	57%	11%	4%	1%
Type I PV Boutons	14%	67%	19%	--	--	26%	70%	4%	--	--
Type II PV Boutons	33%	48%	15%	4%	--	12%	62%	17%	9%	--
Non-PV Boutons	55%	44%	1%	--	--	61%	37%	2%	--	--